JOURNAL OF MATERIALS SCIENCE 23 (1988) 2037–2050

Failure-mechanism maps for engineering polymers

Z. BIN AHMAD
Corporate Planning Department, Sime Derby Berhad, Jalan Raja Lant, 50350 Kuala Lumpur, Malaysia

M. F. ASHBY
Cambridge University Engineering Department, Trumpington Street, Cambridge CB2 1PZ, UK

This paper reports on progress in assembling experimental data and simplified theoretical models for the deformation and fracture of engineering polymers into diagrams which summarize their inelastic response to stress. A number of regimes are identified: brittle fracture initiated by crazing or shear-banding; plasticity terminated by ductile fracture; cold-drawing; rubbery and viscous flow; a regime in which deformation is purely elastic; and one in which adiabatic heating influences deformation. Data for a number of commercial polymers (polymethylmethacrylate, polystyrene, polycarbonate, polyisobutylene and an epoxy resin) are fitted to simplified constitutive equations for each regime. The equations are then used to construct diagrams, one for tension and one for compression, which relate strength to temperature T and strain rate $\dot{\varepsilon}$, over a wide range of these variables.

Nomenclature

C_p	Specific heat ($J\,kg^{-1}\,K^{-1}$).
C_1, C_2	WLF constants.
E	Modulus ($N\,m^{-2}$).
E_0	Modulus at 0 K ($N\,m^{-2}$).
G_c	Fracture energy per unit area ($J\,m^{-2}$).
K_{IC}	Critical stress intensity factor ($N\,m^{-3/2}$).
$K_{IC,0}$	Critical stress intensity factor at 0 K ($N\,m^{-3/2}$).
M_k, M_w, M_n, M_k, M_z, M_i, M_{ref}, M_{cr}	Molecular weights ($kg\,mol^{-1}$).
M_{cr}	Critical molecular weight ($kg\,mol^{-1}$).
R	Universal gas constant ($J\,mol^{-1}\,K^{-1}$).
T, T_0	Temperatures (K).
T_g	Glass transition temperature (K).
T_b	Brittle–ductile transition temperature (K).
T_d	Decomposition temperature (K).
$\tilde{T}$	Normalized temperature (K).
V_p	Pressure activation volume (m^3).
V_s	Shear activation volume (m^3).
a	Thermal diffusivity ($m^2\,sec^{-1}$).
c	Flaw size (mm).
f_g	Fractional free volume at T_g.
K	Bulk modulus ($N\,m^{-2}$).
l	Characteristic dimension (m).
n_i	Number of molecules.
p	Pressure ($N\,m^{-2}$).
t	Heat diffusion time (sec).
z	Mass per chain atom.
α	Fractional difference between compressive and tensile strengths.
α_f	WLF constant.
α_m	Temperature coefficient of the modulus.
β	Pressure coefficient of the yield stress.
δ_c	Critical crack opening displacement (m).
$\delta_{c,m}$, $\delta_{c0,m}$	Critical crack opening displacements for molecular weight. M at temperatures T and 0 K, respectively (m).
ε	Strain.
$\dot{\varepsilon}$	Strain rate (sec^{-1}).
$\dot{\varepsilon}_0$	Pre-exponential for strain rate (sec^{-1}).
ϱ	Density ($kg\,m^{-3}$).
ΔT	Temperature rise (K).
ΔH	Activation energy ($J\,mol^{-1}$).
ΔH_v	Activation energy for viscous flow ($J\,mol^{-1}$).
σ	Stress ($N\,m^{-2}$).
$\tilde{\sigma}$	Normalized stress.
σ_b, σ_y	Brittle and yield strengths, respectively ($N\,m^{-2}$).
σ_c, σ_T	Compressive and tensile stresses, respectively ($N\,m^{-2}$).
$\sigma\,(T, \dot{\varepsilon})$	Temperature- and strain rate-dependent stress ($N\,m^{-2}$).
σ_d	Drawing stress ($N\,m^{-2}$).
σ_f	Fracture stress ($N\,m^{-2}$).
σ_s	Shear stress ($N\,m^{-2}$).
σ_0	Tensile stress at 0 K ($N\,m^{-2}$).

0022–2461/88 $03.00 + .12

$\sigma_{f,0}$, $\sigma_{y,0}$	Fracture stress and yield stress at 0 K, respectively ($N m^{-2}$).
$\sigma_{f0,m}$, $\sigma_{f0,k}$	Fracture stress at 0 K for molecular weights M and M_k, respectively ($N m^{-2}$).
η	Melt viscosity ($N m^{-2} sec$).
η_0	Pre-exponential for viscosity ($N m^{-2} sec$).
η_{T_g}	Viscosity at T_g ($N m^{-2} sec$).
η_{cr}	Critical viscosity ($N m^{-2} sec$).

1. Introduction

Engineering design with polymers requires an understanding of their stiffness and their strength, and the way these depend on temperature and the time or rate of loading. This paper concerns *strength*: the stress at which the polymer deforms plastically or fractures, and the mechanisms by which it does so.

An idea of the range of response is given by Fig. 1, which shows, schematically, how the stress–strain curve of an engineering polymer changes with temperature at constant strain rate. At the lowest temperature it is as brittle as glass, at the highest, as plastic as putty; in between it is ductile and tough. The picture is further complicated by the variable of stress-state: the response in tension differs markedly from that in compression.

Briefly, the known mechanisms of failure are as follows. At temperatures well below the glass transition temperature, T_g, the polymer responds in an almost linear-elastic manner up to the breaking point where it fails by *brittle fracture*. The elastic elongation is only a few per cent and catastrophic fracture occurs suddenly without any indication of plastic yielding, although it is generally thought that it is initiated by localized shear yielding or crazing. Both *shear-banding* and *crazing* are favoured by localization of plastic strain and therefore are common in polymers exhibiting strain-softening characteristics. They are competing mechanisms; the one which dominates depends on the conditions of testing and the structure of the polymer. Crazing is suppressed by compressive stresses and by a high degree of cross-linking; it is favoured by certain environments, giving a link between craze formation and the phenomenon of environmentally-assisted fracture.

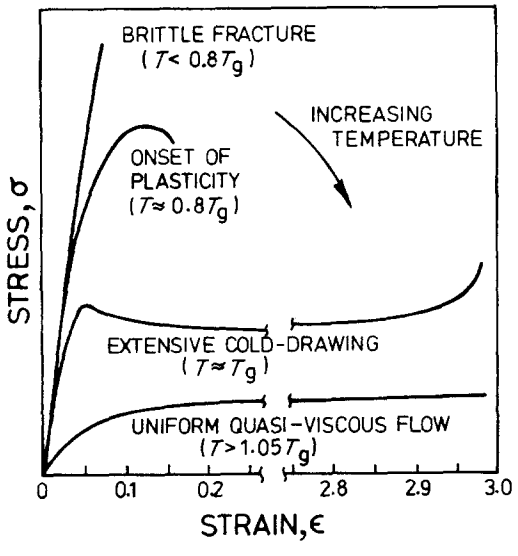

Figure 1 Schematic load–extension curves for a linear polymer at different temperatures. Well below T_g the polymer is brittle. Near T_g it is plastic and may show cold-drawing. Above T_g, it is viscous.

Increasing the temperature changes the mode of fracture from brittle to ductile, characterized by the appearance of a *yield point* where the load falls prior to fracture. The elongation is still comparatively low, sometimes with indications of necking. A further increase in the temperature leads to *necking* and subsequent *cold-drawing* where the extensions are now very large: up to 1000%. The onset of cold-drawing, however, is very much dependent on the stability of the neck and this is governed by the level of strain hardening and, perhaps, by adiabatic heating (discussed later). Finally, at very much higher temperatures, the polymer deforms homogeneously by *viscous flow* with very large extensions. For amorphous polymers this flow behaviour normally occurs at temperatures well above T_g and the corresponding stress levels are very low.

Broadly speaking, each mechanism has a characteristic range of temperature, stress and strain rate in which it is dominant. When the stress is normalized by the modulus and the temperature by the glass transition temperature the fields of dominance of a given mechanism for a number of polymers are brought into approximate coincidence. So in formulating equations to describe the flow and fracture mechanisms, it makes sense to express them in terms of the normalized variables:

$$\tilde{\sigma} = \sigma/E_0 \quad (1)$$

$$\tilde{T} = T/T_g \quad (2)$$

The modulus E itself depends on temperature. Within the glassy regime ($T < 0.9\,T_g$) this temperature dependence can be approximated by

$$E = E_0\left(1 - \alpha_m \frac{T}{T_g}\right) \quad (3)$$

where α_m is a dimensionless temperature coefficient. Data for E_0, T_g and α_m are assembled in Table I.

We now examine the mechanisms in more detail, identifying a simplified constitutive equation (an equation relating stress, temperature, strain rate and material properties) for each. Throughout the paper we use the abbreviations for the polymer names given in Table I.

2. Mechanisms of failure

2.1. Brittle fracture

Low temperatures ($\lesssim 0.8\,T_g$) or high strain rates favour brittle fracture (Fig. 2). If the polymer contains incipient cracks or flaws (crack length = $2c$) then fracture occurs in tension when, roughly speaking, the Griffith criterion [14] is satisfied, that is when the tensile stress exceeds

$$\sigma_f = K_{IC}/(\pi c)^{1/2} \quad (4)$$

Equation 4 implies that the fracture stress increases

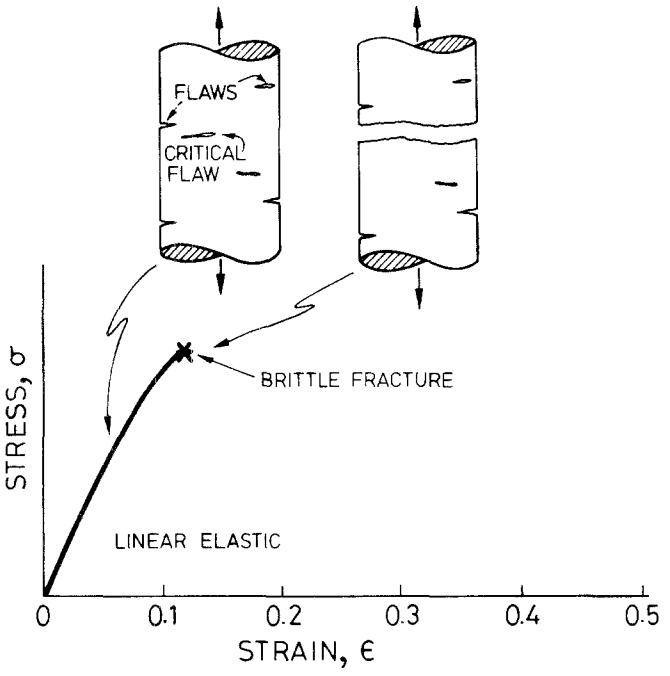

Figure 2 Schematic diagram illustrating brittle fracture. It is typical of the temperature range below $0.8T_g$. A crack nucleates at a pre-existing flow or craze and propagates unstably.

with decreasing flaw size, but for polymers it is found that there is a critical flaw size below which the fracture stress becomes independent of the size of flaws which have been deliberately introduced [15, 16]. This leads to the conclusion that polymers contain natural defects which behave like flaws, or that the application of stress in some way creates them. At room temperature the critical flaw sizes for PS and PMMA are about 1 mm and 0.05 mm, respectively [15]. The general view is that a naturally occurring defect in an unnotched sample is a craze or a shear band (both of which have crack-like stress fields associated with them) and that the tensile strength of the brittle regime is given by Equation 4 with c set equal to the typical value. The brittle-fracture strength in compression is much larger–a factor of between 10 and 15 times–because crack growth in compression, though possible, is much more difficult [17]. For many polymers this compressive fracture strength is so large that another mechanism (plasticity) operates instead.

We are interested in the way in which the fracture strength varies with temperature and rate of loading. It is known that K_{IC} for some polymers, at least, depends on these variables, but that the critical crack-opening displacement, δ_c, does not [18–21]. Since δ_c can be written as $K_{IC}^2/E\sigma_y$ it follows that

$$\frac{K_{IC}^2}{E\sigma_y} = \frac{K_{IC,0}^2}{E_0\,\sigma_{y,0}} \tag{5}$$

where subscript 0 refers to the value at a reference temperature, T_0. Assuming that the incipient crack length c remains constant, Equations 4 and 5 give

$$\frac{\sigma_f}{E_0} = \frac{\sigma_{f,0}}{E_0}\left(\frac{E}{E_0}\frac{\sigma_y}{\sigma_{y,0}}\right)^{1/2} \tag{6}$$

where the stresses have been normalized with E_0. Taking the reference temperature T_0 as 0 K and using Equation 3 gives

$$\frac{\sigma_f}{E_0} = \frac{\sigma_{f,0}}{E_0}\left[\frac{\sigma_y}{\sigma_{y,0}}\left(1 - \alpha_m\frac{T}{T_g}\right)\right]^{1/2} \tag{7}$$

Values of the normalized fracture stress at 0 K, $\sigma_{f,0}/E_0$, are listed in Table II. Values of α_m were given in Table I. The yield strength ratio $\sigma_y/\sigma_{y,0}$ is discussed in the next section.

In the truly brittle regime, a single craze or shear band may be all that is required to trigger fracture. But at temperatures near $0.8\,T_g$, crazing (Fig. 3) becomes more general and may even allow a certain amount of "plastic" deformation. A craze is a crack-like region consisting of an interpenetrating system of voids and drawn polymer fibrils. But unlike a true crack, load is transmitted across the craze faces by the fibrils. The initiation of a crack from the craze occurs when the fibrils break down (Fig. 3). Because of this, crazes can grow in a stable way giving a limited amount of additional strain (for a review see Kinlock and Young [27]; for stress-criteria for crazing see Sternstein and Ongchin [28] and Oxborough and Bowden [29]; and for the effect of environment in

TABLE I Data for E_0, T_g and α_m

Polymer	E_0 (GPa)	T_g (K)	α_m
Polymethylmethacrylate (PMMA)	8.57 [1, 2]	378 [3–5]	0.28 [1, 2]
Polystyrene (PS)	6.30 [1, 2, 8, 9]	373 [3–5]	0.28 [8, 9]
Polycarbonate (PC)	7.25 [1, 2]	423 [10]	0.30*
Polyisobutylene (PIB)	7.90†	203 [11]	0.28*
Epoxy resin (EP)	5.30 [12]	423 [12, 13]	0.31 [12]

*Assumed values.
†Estimated from data of Schmeider and Wolf [7].

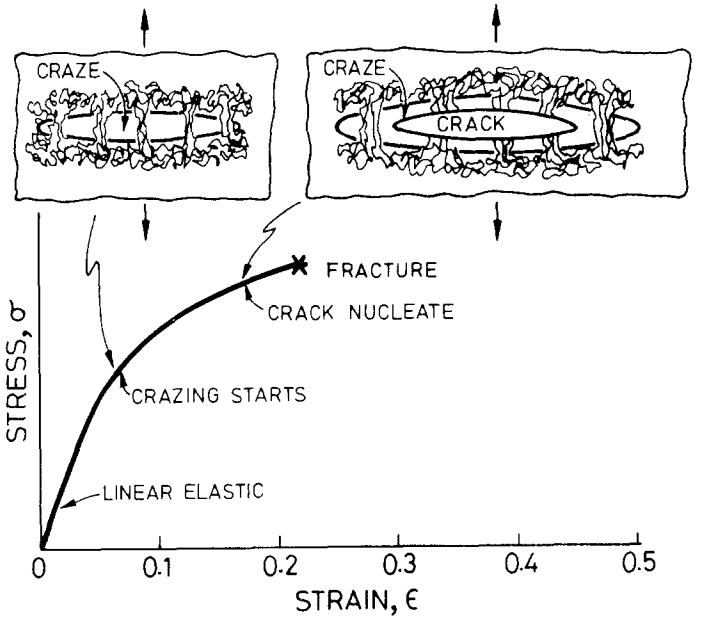

Figure 3 Schematic diagram showing crazing and the nucleation of a crack within a craze. Near $0.8T_g$, crazing can be general, giving significant inelastic extension before fracture.

stimulating crazing see Andrews and Bevan [30] Rabinowitz and Beardmore [31], Brown [32] and Wu and Brown [25]).

2.2. Plasticity

True plasticity starts, in most commercial polymers, at around $0.8\,T_g$ in tension, but extends to much lower temperatures in compression. Large plastic strains in compression are possible by shear banding (Fig. 4) and this mechanism can operate in tension also. But it is also common in linear polymers to find that plasticity in tension results from cold-drawing: a very non-homogeneous deformation, during which the polymer molecules align themselves with the tensile axis (Fig. 5).

The temperature dependence of the fracture strength, σ_f, and of the plastic strength, σ_y, differ: usually the plastic strength (which we review in a moment) falls faster. Then, for a given strain rate, stress state and sample geometry (simple tension of a round bar, for example) there exists a characteristic temperature – the ductile–brittle transition temperature – at which the two strengths are equal. Below this temperature σ_f is lower than σ_y and the preferred failure mode is brittle. Above, plasticity leading to a ductile fracture becoming the dominant mechanism. Table III gives some typical values of the transition temperatures T_b corresponding to strain rates of the order of 10^{-3} sec^{-1}, for unnotched samples in tension. For polystyrene, T_b and T_g are almost the same, leading Vincent [24] to suggest that there is a partial correlation between the yield process and the molecular relaxations that govern the tensile modulus. Similarly, for polycarbonate, the low transition temperature has been attributed to the secondary relaxations that occur at two temperatures [34].

In a ductile regime, polymers show a yield stress followed by a constant drawing or shearing plateau as shown schematically in Figs 4 and 5. Both the yield stress and the drawing stress depend on temperature, strain rate and hydrostatic pressure. For polymers it is found that the compressive yield stress is always greater than the tensile yield stress. This implies that the usual Tresca and Von Mises yield criteria are not adequate to describe their yield behaviour, which depends on hydrostatic pressure [35–37]. A number of workers [37–47] have developed molecular models for yield and drawing. Almost all are based on extensions of the Eyring equation following the lines developed to describe plastic flow in metals (see, for example, Kocks *et al.* [48]). When suitably recast, almost all the models reduce approximately to the equation

$$\dot{\varepsilon} = \dot{\varepsilon}_0 \exp\left[-\left(\frac{\Delta H - \sigma_s V_s + pV_p}{RT}\right)\right] \quad (8)$$

where ΔH is the activation energy for the unit flow process and $\dot{\varepsilon}_0$ is an adjustable pre-exponential constant. Equation 8 can be rearranged in the form

$$\dot{\varepsilon} = \dot{\varepsilon}_0 \exp -\frac{\Delta H}{RT}\left(1 - \frac{\sigma_y}{\sigma_{y,0}} + \beta\frac{p}{K}\right) \quad (9)$$

We now define the fractional difference between the

TABLE II Normalized fracture stress at 0 K

Polymer	$\sigma_{f,0}/E_0$
PMMA	0.021*
PS	0.0165†
PC	0.023‡
PIB	0.021§
EP	0.021¶

*Extrapolated, using data of Beardmore [22], Imai and Brown [23], Morgan and Ward [20] and Vincent [24].
†Extrapolated, using data of Wu and Brown [25].
‡Extrapolated, using data of Bauwens-Crowet *et al.* [26].
§Assumed.
¶Extrapolated, using data of Pink and Campbell [12].

TABLE III Brittle–ductile transition temperature (T_b)

Polymer	T_b (K)
PMMA	318 [33]
PC	73 [33]
PS	363 [33]
EP	73 [12]

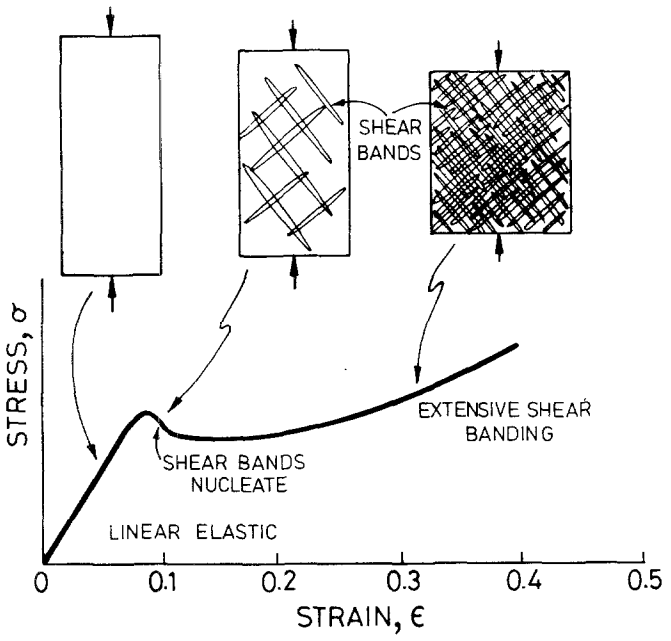

Figure 4 Shear yielding by the formation of localized bands or packets of shear.

compressive and tensile strength as

$$\alpha = \frac{2(\sigma_c - \sigma_T)}{(\sigma_c + \sigma_T)} \tag{10}$$

Using Equation 10 we can invert Equation 9 to give

$$\frac{\sigma_y}{E_0} = \frac{\sigma_{y,0}}{E_0}\left(\frac{2 \pm \alpha}{2}\right)\left[1 + \left(\frac{RT_g}{\Delta H}\right)\left(\frac{T}{T_g}\right)\ln\left(\frac{\dot{\varepsilon}}{\dot{\varepsilon}_0}\right)\right] \tag{11}$$

where the positive sign gives the compressive strength and the negative sign gives the tensile strength. Some polymers (see Ward [49]) obey the simple equation well. Others require a summation of two Eyring terms to give a complete description [50]. We will use the simple Equation 11 in constructing the maps which follow. We have fitted data from various sources to it to determine the constants. They are tabulated in Table IV.

2.3. Viscous flow

At sufficiently high temperatures ($T \gtrsim 1.1T_g$) polymers deform by viscous flow. This is the regime in which the injection moulding and forming of linear polymers is performed. Within it, the stress is related to the strain rate by

$$\frac{\sigma}{E_0} = \frac{3\dot{\varepsilon}\eta}{E_0} \tag{12}$$

where η is the melt viscosity.

There have been numerous theories proposed to describe the temperature-dependence of the viscosity in this regime (for a review see Kumar, [53]). At the highest temperatures it follows an Arrhenius law:

$$\eta = \eta_0 \exp\left[\frac{\Delta H_v}{RT_g}\left(\frac{T_g}{T} - \frac{T_g}{T_0}\right)\right] \tag{13}$$

where η_0 is the viscosity at a reference temperature T_0. Equation 13 is useful only for a limited range of

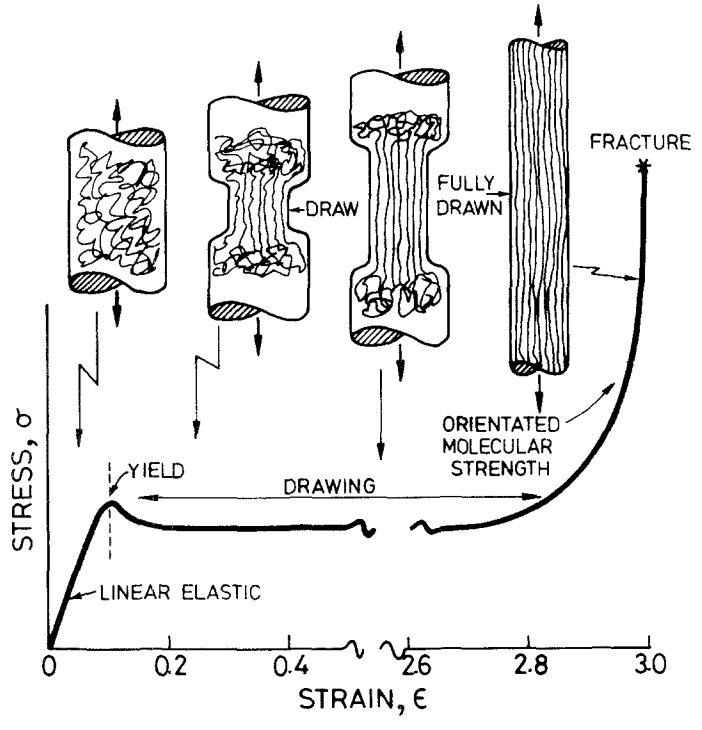

Figure 5 Schematic diagram illustrating yield followed by cold-drawing. Extensions are large.

TABLE IV Yield and drawing data

Polymer	α	$\sigma_{y,0}/E_0$	$\dot{\varepsilon}_0$ (sec^{-1})	$\Delta H/RT_g$
PMMA*	0.288	0.045	6×10^{10}	33
PS†	0.30	0.038	1×10^{16}	52
PC‡	0.20	0.023	3×10^{14}	46
PIB§	0.288	0.045	6×10^{10}	33
EP¶	0.10	0.024	1×10^{15}	45

*Extrapolated, using data of Vincent [24], Beardmore [22], Imai and Brown [23] and Morgan and Ward [20].
†Extrapolated using data of Argon *et al.* [51], Bowden and Raha [52] and Wu and Brown [25].
‡Extrapolated, using data of Bauwens-Crowet *et al.* [26].
§Assumed.
¶Extrapolated, using data of Pink and Campbell [12].

temperatures because, near T_g, the activation energy ΔH_v itself depends on the temperature [54, 55]. Near T_g, a better description [56] is given by

$$\eta = \eta_0 \exp \frac{-2.303C_1(T - T_0)}{C_2 + T - T_0} \quad (14)$$

In using this equation it is common to take the reference temperature to be T_g itself, when the constants C_1 and C_2 have the values 17.4 and 51.6 K, respectively (though these should only be used in the absence of experimentally determined values), and η_0 then becomes η_{T_g}. It is found that Equation 14 fits the experimental data quite well, and it is this equation which we have used in constructing the diagrams shown later. Values of η_{T_g}, C_1 and C_2 are listed in Table V.

As the temperature is raised further, a characteristic value T_d is reached at which chemical decomposition of the polymer occurs. Absolute and normalized values of T_d are given in Table VI.

2.4. Adiabatic heating

The tensile behaviour of polymers is complicated by their low thermal conductivities. The heat generated during plastic deformation accumulates within a localized region of the specimen, causing local softening. At low rates of loading, the heat is conducted away sufficiently rapidly that the temperature rise is unimportant. But as the loading rate is increased, less time is available for conduction and the local temperature in a shear band rises. The heat is conducted into the unyielded material on either side of the sheared zone, thereby reducing its yield strength and giving strain-softening. With increased strain-softening, necking takes place and, coupled with the reduced local yield stress, the neck is able to propagate to give cold-drawing. Marshall and Thompson [59] have used this

TABLE V Flow viscosity parameters

Polymer	η_{T_g} ($N\,m^2\,sec$)	C_1	C_2 (K)
PMMA	9×10^{15}*	20.9 [57]	58 [57]
PS	3×10^{14}*	14.5 [57]	50.4 [57]
PC	1.5×10^{16}*	17.4 [57]	51.6 [57]
PIB	9×10^{15}†	17.4 [57]	51.6 [57]
EP	–	–	–

*Best fit of experimental data.
†Assumed.

TABLE VI Decomposition temperatures

Polymer	T_d/T_g	T_d (K)
PMMA	1.44 [58]	544 [58]
PS	1.46 [58]	545 [58]
PC	1.50*	635*
PIB	3.07 [11]	623 [11]
EP	1.50*	635*

*Assumed.

idea to explain cold-drawing in polyethylene terephthalate; but it has generality and all polymers, under the right circumstances, will show adiabatic heating effects.

For significant adiabatic heating two conditions must be met. First, assuming no heat loss, the plastic work, $\sigma_d\varepsilon$, per unit volume (where σ_d is the drawing stress) must be sufficient to raise the temperature significantly. The energy associated with raising the temperature of the polymer, per unit volume, by ΔT is $\Delta TC_p\varrho$. For no heat loss we therefore have the condition

$$\sigma_d\varepsilon = \Delta TC_p\varrho \quad (15)$$

We will assume that a temperature rise of 10° C or more will significantly change the properties of the polymer. Then, from Equation 15, the first condition for adiabatic heating is that the drawing stress must be greater than the critical value:

$$\sigma_d > 10C_p\varrho/\varepsilon \quad (16)$$

This is a necessary, but not a sufficient, condition for adiabatic heating to be important. If the strain rate is low, the heat generated by the plastic deformation is conducted away and thus the temperature does not rise significantly. The second condition is that the time taken to insert the plastic work is small compared to the characteristic heat diffusion time. The heat diffusion time is defined as

$$t = l^2/2a$$

where a is the thermal diffusivity and l is a characteristic dimension of the sample, which we assume to be the distance from the centre of the sample to the nearest heat sink. If the average strain in the sample is unity, then the second condition for adiabatic heating is that the strain rate exceed the value

$$\dot{\varepsilon} > 2a/l^2 \quad (17)$$

Data for density, specific heat and thermal diffusivity are given in Table VII. Using these data, and assuming an average strain of unity, we find that adiabatic heating requires, from the first condition,

$$\frac{\sigma_d}{E_0} \gtrsim 2 \times 10^{-3} \quad (18)$$

and that the second condition imposes the requirement on strain rate of

$$\varepsilon \gtrsim 10^{-3}\,sec^{-1} \quad (19)$$

These two conditions now define an area, shown as a shaded zone on later diagrams, in which adiabatic heating is significant. It is worth noting that Allison

TABLE VII Thermal properties

Polymer	Density ($kg\,m^{-3}$)	Specific heat ($J\,kg^{-1}\,K^{-1}$)	Thermal diffusivity ($m^2\,sec^{-1}$)
PMMA	1.2×10^3	1500	1.1×10^{-7}
PS	1.1×10^3	1400	0.9×10^{-7}
PC	–	–	–
PIB	0.9×10^3	1600	1.0×10^{-7}
EP	1.5×10^3	1850	1.2×10^{-7}

and Ward [60] show a drop in the drawing stress for polyethylene terephthalate for strain rates greater than $10^{-3}\,sec^{-1}$, which is in general agreement with this calculation. The yield strength, however, does not show this drop because the strains at yield are much smaller (the plastic strain may be as little as 1%) so that the limit set by Equation 16 is increased.

3. The influence of molecular weight on failure mechanisms

Polymer properties depend on molecular weight, M_w. First, the modulus E_0 and the glass temperature T_g both tend to increase with M_w. But even if strengths are normalized by E_0 (as we do in Section 4), a further dependence on molecular weight remains. It is not fully understood, though it must partly reflect the fact that at a crack tip, or within a craze or a shear band, short molecules (low M_w) unravel and separate more readily than longer ones. The incomplete physical understanding can be compensated for by developing empirical modifications of the constitutive equations to build into them a dependence on M_w, and it is of the greatest value to do so: then, data obtained from a batch of polymer with one M_w can be used to predict the properties of a batch with a different M_w. An example of this procedure is given in Section 4.

We now consider briefly the molecular-weight dependence of the important properties and failure mechanisms. We define the weight-average molecular weight as

$$M_w = \frac{\sum n_i M_i^2}{\sum n_i M_i}$$

where n_i is the number of molecules of molecular weight between M_i and M_{i+1}, and the sums are taken over all i.

3.1. The dependence of the modulus on M_w

The glassy modulus reflects the intrinsic stiffness of the secondary bonds in the polymer; and this is not influenced by molecular weight (that is why all linear amorphous polymers have roughly the same glassy modulus). We shall take E_0 to be independent of M_w. The rubbery modulus (that above T_g), on the other hand, depends strongly on M_w. A large molecular weight gives a broad rubbery plateau; reducing M_w reduces or removes it entirely [61].

TABLE VIII Values of $T_{g,\infty}$, A and B (after Fedors [62])

Polymer	$T_{g,\infty}$ (K)	A ($kg\,kmol^{-1}$)	B ($kg\,kmol^{-1}$)
PMMA	387	1.7×10^8	2800
PS	373	1.0×10^8	378
PC	436	2.59×10^8	1270
EP	–	–	–

3.2. The dependence of the glass transition temperature on M_w

The dependence of the glass transition temperature, T_g, on the molecular weight, M, of the polymer is given [62] by

$$T_g = T_{g,\infty} - \frac{A}{M + B} \quad (20)$$

where $T_{g,\infty}$ is the limiting glass transition temperature of the polymer of infinite molecular weight and A and B are material constants whose values depend on the chemical structure of the polymer. Values of $T_{g,\infty}$, A and B are listed in Table VIII.

3.3. The dependence of fracture properties on M_w

The influence of molecular weight on the fracture behaviour of polymers has been widely investigated [21, 63–70]. Below a critical value M_k of the molecular weight, fracture parameters such as the fracture energy, crazing stress and crack opening displacement depend on M_w; above, they do not. Fig. 6 shows examples of this for the three linear polymers which concern us here: PMMA, PS and PC. The effect has been linked to the stress for crazing, which varies more rapidly with M_w than the yield stress does [68, 70], suggesting that the craze stress is dependent on the rate at which disentanglement of the network structure can occur. Donald [70] suggested that low molecular weight polymers with a low entanglement density (such as PS) would possess a higher transition temperature (crazing-to-yield) than samples of high molecular weight. The reverse is true for polymers with a high entanglement density such as PC. Data for the critical molecular weight are summarized in Table IX.

The constitutive equation for fracture (Equation 7) was based on the experimental observation that the critical crack opening displacement (unlike K_{IC} or G_{IC}) was independent of temperature and loading rate. It is

TABLE IX Critical molecular weights, M_k

Polymer	M_k ($kg\,kmol^{-1}$)	Typical molecular weight ($kg\,mol^{-1}$)
PMMA	2×10^5 [69]; 1.5×10^5 [65]	1×10^5 [55]; 4×10^6 [72]
PS	2×10^5 [70]; 1.6×10^5 [65]	2.5×10^5 [54]; 3.6×10^5 [72]
PC	1.5×10^4 [71]*	3×10^4 [54]; 3.5×10^4 [72]
EP	–	3500 [13, 73]

*Based on the dependence of fracture stress on the viscosity-average molecular weight, M_v.

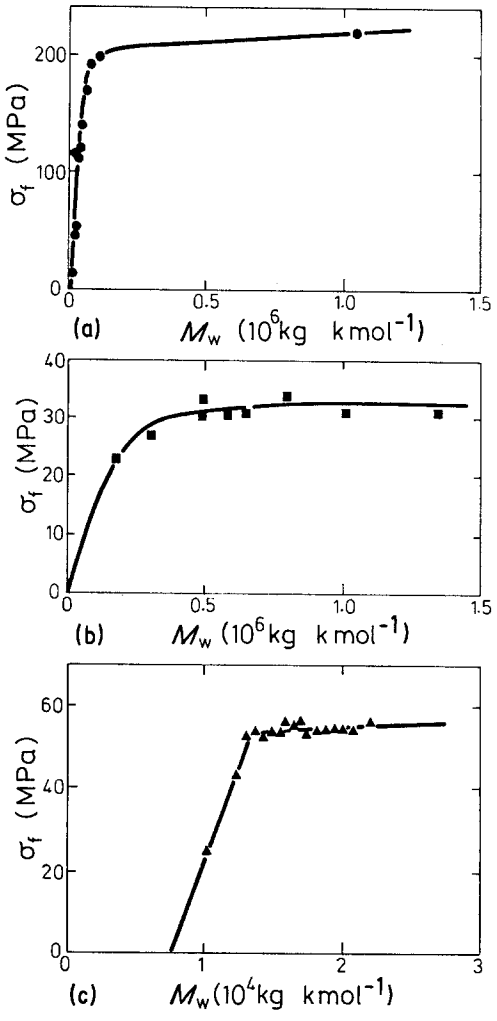

Figure 6 The dependence of the fracture strength on molecular weight for (a) PMMA, (b) PS and (c) PC (after Kinloch and Young, [27]).

known to depend on M_w in much the same way that the fracture strength does (Fig. 6) [69, 74]:

$$\delta_{c,m} \propto M_w \quad \text{if} \quad M_w < M_k \tag{21a}$$

and

$$\delta_{c,m} = \text{constant} \quad \text{if} \quad M_w \geqslant M_k \tag{21b}$$

where $\delta_{c,m}$ is the critical crack opening displacement corresponding to a molecular weight, M_w. Using the standard results $\delta_c = K_{IC}^2/E\sigma_y$ and $K_{IC}^2 = \pi c\sigma_f^2$ gives

$$\sigma_{f,m} = \left(\frac{\delta_{c,m}E\sigma_y}{\pi c}\right)^{1/2} \tag{22}$$

The glassy modulus, E, does not depend on molecular weight; nor does σ_y (see next section). Then the fracture strength corresponding to a given molecular weight is related to that at the critical molecular weight (using Equations 21 and 22) by

$$\sigma_{f,m} = \sigma_{f,k}\left(\frac{M_w}{M_{cr}}\right)^{1/2} \quad \text{if} \quad M_w < M_k \tag{23a}$$

$$\sigma_{f,m} = \sigma_{f,k} \quad \text{if} \quad M_w \geqslant M_k \tag{23b}$$

In constructing diagrams shown later, the fracture strength at the critical molecular weight was obtained from plots like Fig. 6, and then corrected to the new molecular weight using Equations 23.

TABLE X Critical molecular weight, M_{cr}, (after van Krevelen [55])

Polymer	M_{cr} (kg kmol^{-1})
PMMA	3.0×10^4
PS	3.5×10^4
PC	3.0×10^3
EP	–

3.4. The dependence of yield strength on M_w

The yield strength of a linear polymer, at a given fraction of T_g, is essentially independent of molecular weight [68, 70]. We may then use Equation 11, which is expressed in terms of T/T_g, without change.

3.5. The dependence of viscous flow on M_w

The polymer viscosity, η, depends on the molecular weight, M_w, in one of two ways. Below a critical molecular weight, M_{cr}, (which differs from that of Table IX) the viscosity is proportional to the molecular weight so that

$$\eta = \eta_{cr}\left(\frac{M_w}{M_{cr}}\right) \tag{24a}$$

where η_{cr} is the viscosity of a melt with molecular weight M_{cr}. Above M_{cr}, the dependence changes such that

$$\eta = \eta_{cr}\left(\frac{M_w}{M_{cr}}\right)^{3.4} \tag{24b}$$

Data for M_{cr} are listed in Table X.

We have used this information to adapt the equation for viscous flow (Equation 12 with Equation 14) to include molecular weight. Most commercial polymers have molecular weights that are larger than M_{cr}; then, in the range $M > M_{cr}$, Equation 24b is used to modify Equation 14. When extrapolating to molecular weights below M_{cr}, Equation 24a is used for the part of the extrapolation for which $M < M_{cr}$. The procedure sounds cumbersome when expressed in words, but it is simple to include in the numerical procedure for constructing failure-mechanism diagrams, which we now describe.

4. Failure-mechanism diagrams

4.1. Construction of the diagrams

Polymers, we have seen, fail by one of a number of competing mechanisms: brittle fracture, plastic collapse, viscous deformation and so forth. Each can be described by a constitutive equation with the general form

$$\frac{\sigma}{E_0} = f(\dot{\varepsilon}, T/T_g, \text{stress state, molecular weight}) \tag{25}$$

where σ is the "failure strength"; we called it σ_f for brittle fracture, σ_y for plastic yielding and σ_v for viscous flow. For a given $\dot{\varepsilon}$, T/T_g, stress state and molecular weight, one mechanism will allow failure at a lower stress than any other. We define this as the *dominant mechanism*, and the *failure strength* is given by

$$\frac{\sigma}{E_0} = \text{least of}\left(\frac{\sigma_f}{E_0}, \frac{\sigma_y}{E_0}, \frac{\sigma_v}{E_0}\right) \tag{26}$$

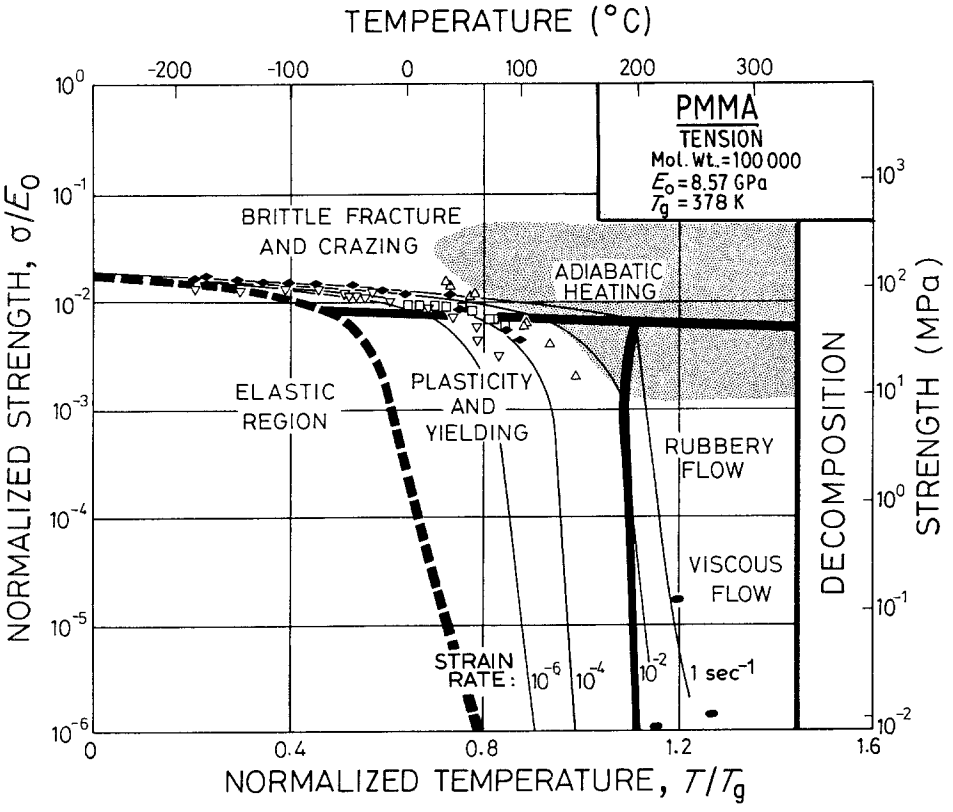

Figure 7 A failure-mechanism diagram for PMMA (mol. wt. = 10^5 kg mol^{-1}), E_0 = 8.57 GPa, T_g = 378 K) of elastic deformation ($\dot{\varepsilon} < 10^{-12}$ sec^{-1}), brittle fracture, plasticity and viscous flow. (△) Vincent [63], (▽) Beardmore [22], (◆) Imai and Brown [23], (□) Morgan and Ward [20], (●) Brodnyan *et al.* [75].

It is attractive to have an overall picture of the way in which a given polymer responds to stress. One format for presenting this is as a failure-mechanism diagram, of which Figs 7 to 15 below are examples. The axes are the normalized failure strength σ/E_0 and the normalized temperature T/T_g. Each diagram is divided into *fields* within which a single mechanism is dominant; the field boundaries (heavy lines) are the loci of points at which two mechanisms have equal failure strengths. Superimposed on the fields are *contours of constant strain rate*, $\dot{\varepsilon}$. A diagram for a given polymer and stress state is constructed by the simple

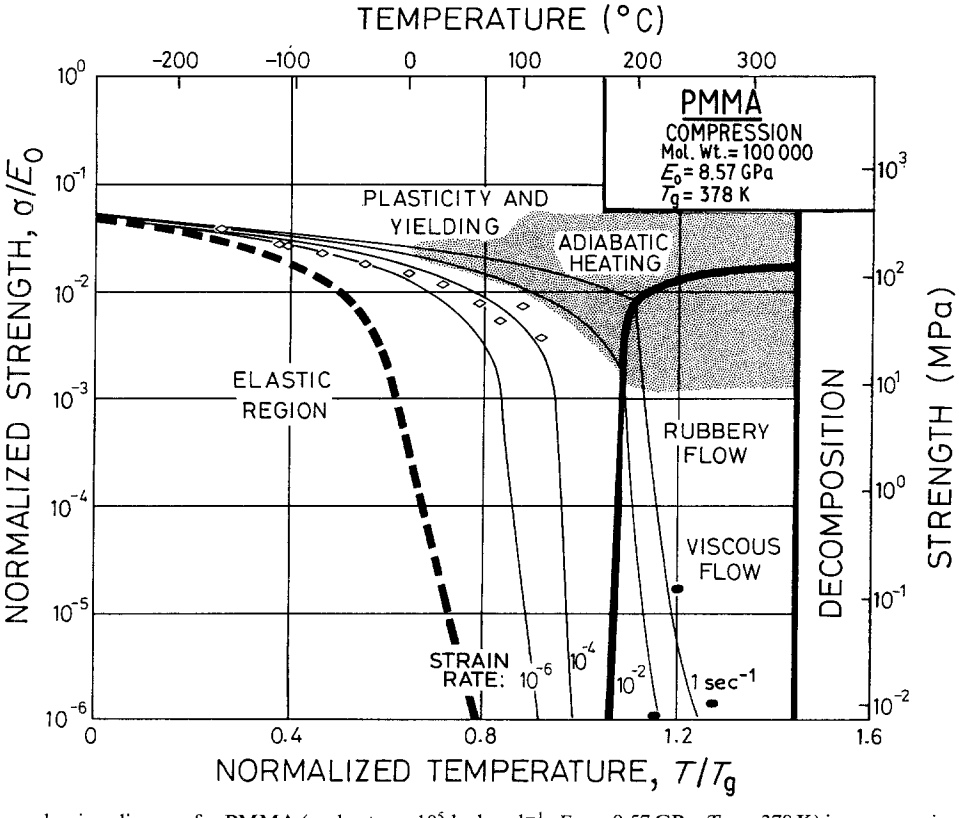

Figure 8 A failure-mechanism diagram for PMMA (mol. wt. = 10^5 kg kmol^{-1}, E_0 = 8.57 GPa, T_g = 378 K) in compression. Brittle fracture is suppressed in unnotched samples. (◇) Beardmore [22], (●) Brodnyan *et al.* [75].

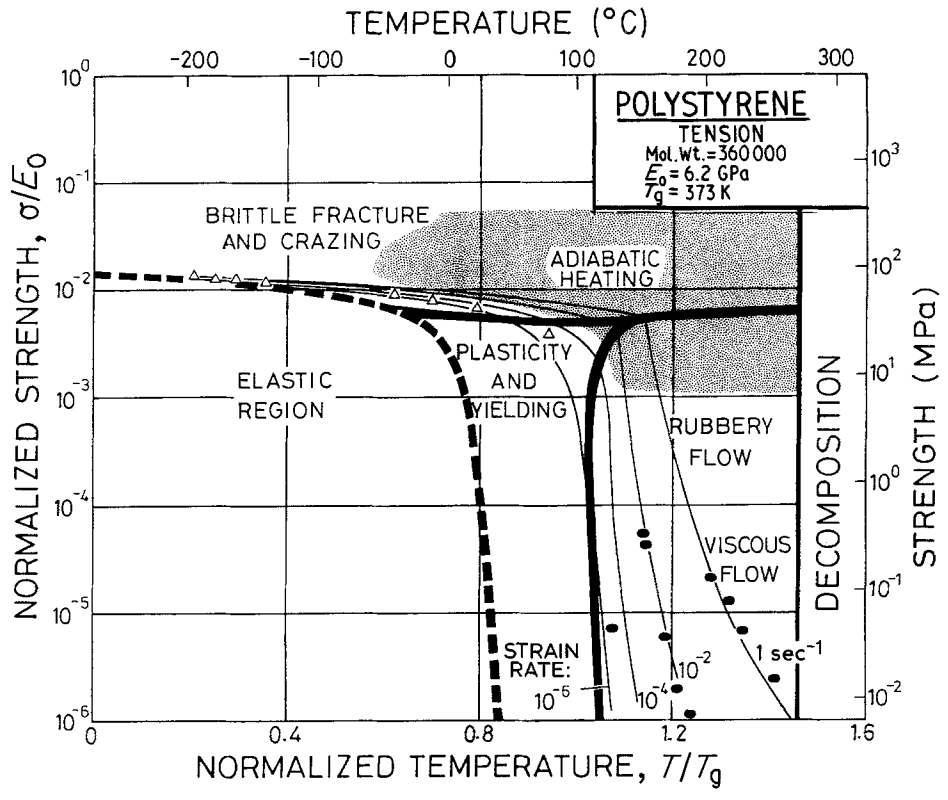

Figure 9 A failure-mechanism diagram for polystyrene (mol. wt. = 3.6×10^5 kg kmol^{-1}, E_0 = 6.2 GPa, T_g = 373 K) in tension. It shows regimes of elastic, brittle, plastic and viscous behaviour. (△) Wu and Brown [25] (1.7×10^{-4} sec^{-1}), (●) Spencer and Dillon [76].

numerical procedure of evaluating each of the set of constitutive equations, using the data for the polymer given in Sections 2 and 3 and using Equation 26 to select the strength. The field boundaries (full heavy lines) are found by locating the stress and temperature at which a change in dominant mechanism takes place. The heavy broken lines correspond to the contour at a strain rate of 10^{-12} sec^{-1}. Since it is difficult to make measurements at strain rates lower than this, we have chosen this contour to describe the boundary between the elastic region (at low temperatures) and the yield regime. The regime of adiabatic heating is

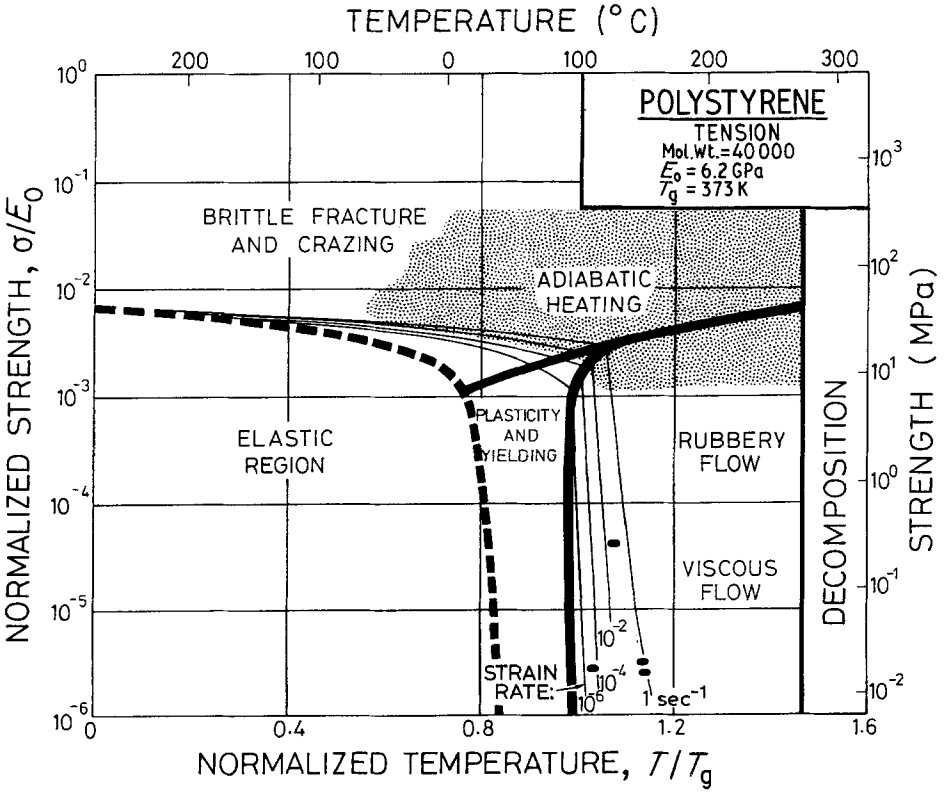

Figure 10 A failure-mechanism diagram for polystyrene (mol. wt. = 4×10^4 kg kmol^{-1}, E_0 = 6.2 GPa, T_g = 373 K) in tension. The regime of plasticity is reduced in extent. (●) Spencer and Dillon [76].

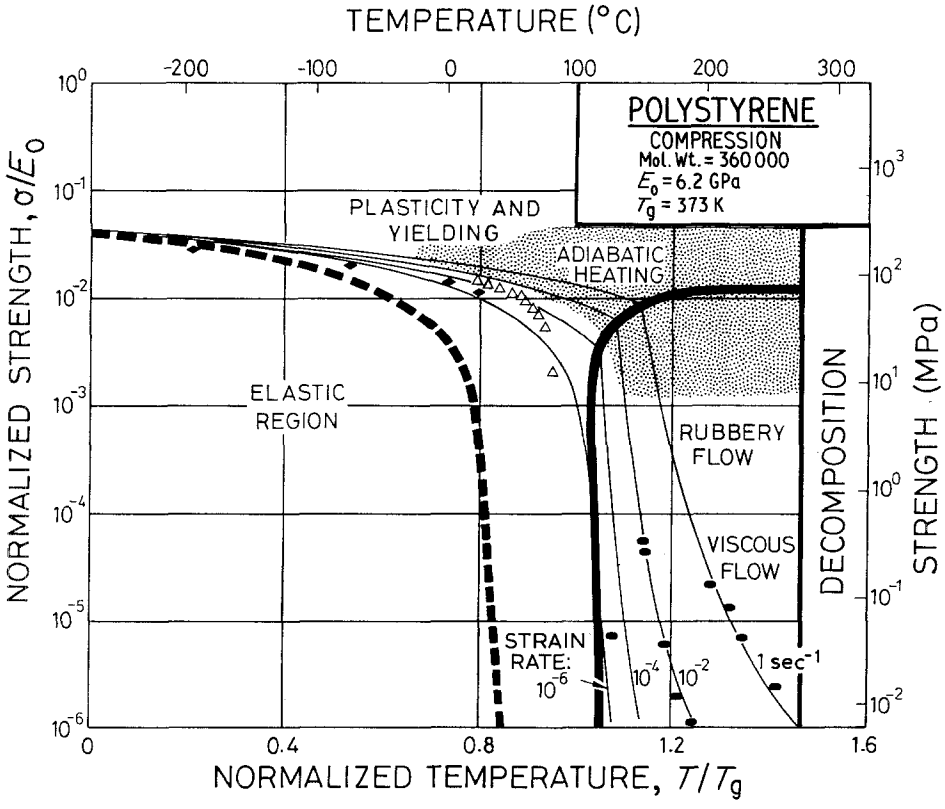

Figure 11 A failure-mechanism diagram for polystyrene (mol. wt. = 3.6×10^5 kg kmol^{-1}, E_0 = 6.2 GPa, T_g = 373 K) in compression. Brittle fracture is suppressed in unnotched samples. (△) Bowden and Raha [52] (3.6×10^{-4} sec^{-1}), (◆) Argon *et al.* [51] (3.1×10^{-3} sec^{-1}), (●) Spencer and Dillon [76].

shown as a shaded zone, bounded by Equations 18 and 19. The viscous flow regime is subdivided roughly into the regime of rubber flow and that of true viscous deformation.

Data for the fracture, flow, and viscous strengths, from various published sources, are plotted on the diagrams. (Many of the parameters of the constitutive equations listed in the earlier tables were determined by fitting them to these data.) They give an idea of the accuracy with which the models fit the data. In cases where the molecular weight of the test samples was not stated, we have assumed typical values.

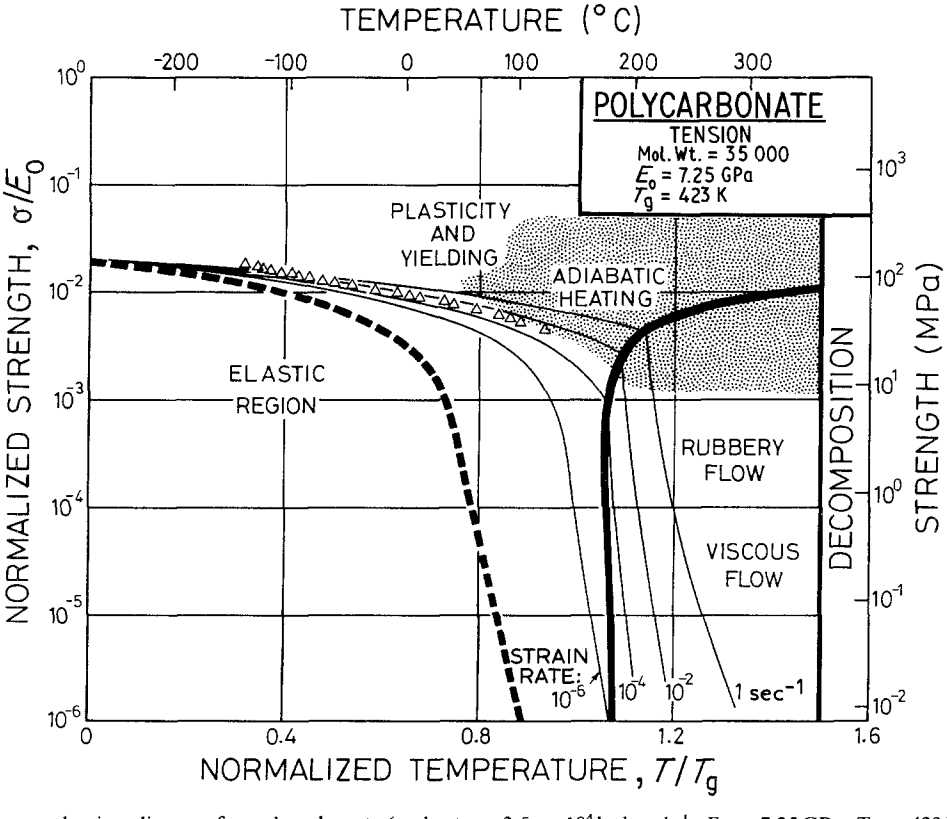

Figure 12 A failure-mechanism diagram for polycarbonate (mol. wt. = 3.5×10^4 kg kmol^{-1}, E_0 = 7.25 GPa, T_g = 423 K) in tension. PC with this molecular weight shows plasticity in tension. (△) Bauwens-Crowet *et al.* [26] (4.2×10^{-3} sec^{-1}).

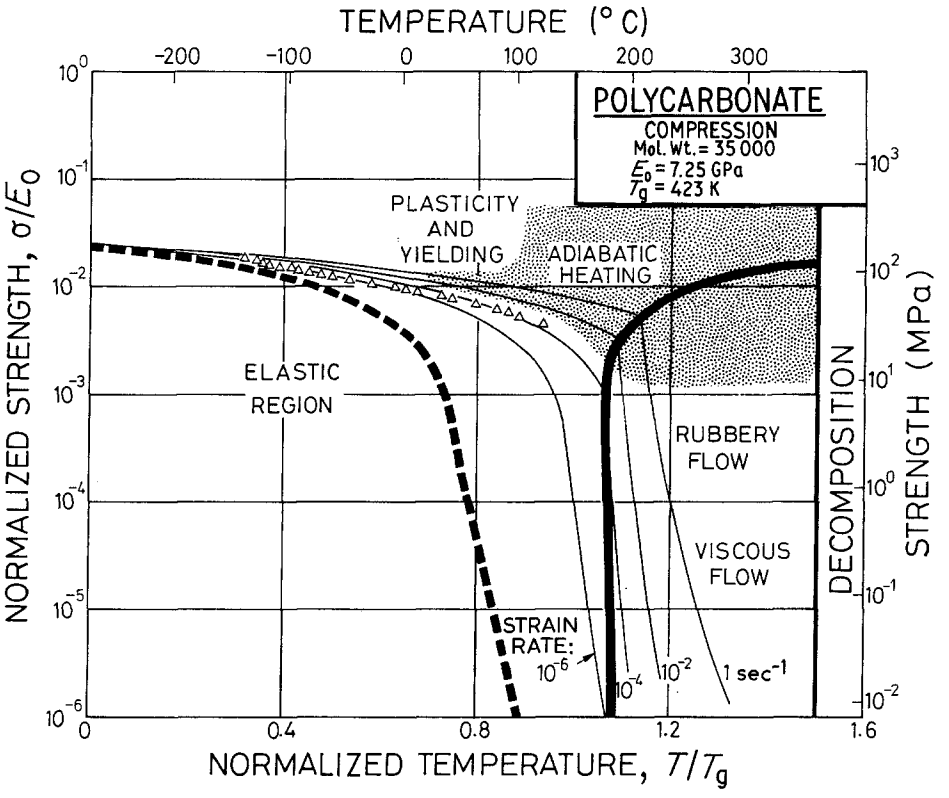

Figure 13 A failure-mechanism diagram for polycarbonate (mol. wt. = 3.5×10^4 kg kmol^{-1}, E_0 = 7.25 GPa, T_g = 423 K) in compression. The stress level for a given strain rate is slightly higher than for tension. (△) Bauwens-Crowet *et al.* [26] (4.2×10^{-3} sec^{-1}).

This approach contains, of course, many assumptions and approximations. The details of the rate-dependence of crazing (which is thought to trigger brittle fracture), of the differences between shear yielding and cold drawing and of the ways in which mechanisms interact, have been neglected and merit much more detailed study. But despite this, the diagrams (described next) show a pattern and consistency which encourages the view that they are the first step in building an overall picture of polymer deformation.

4.2. Features of the diagrams

Figs 7 and 8 show the behaviour of PMMA in tension and compression respectively. The molecular weight is

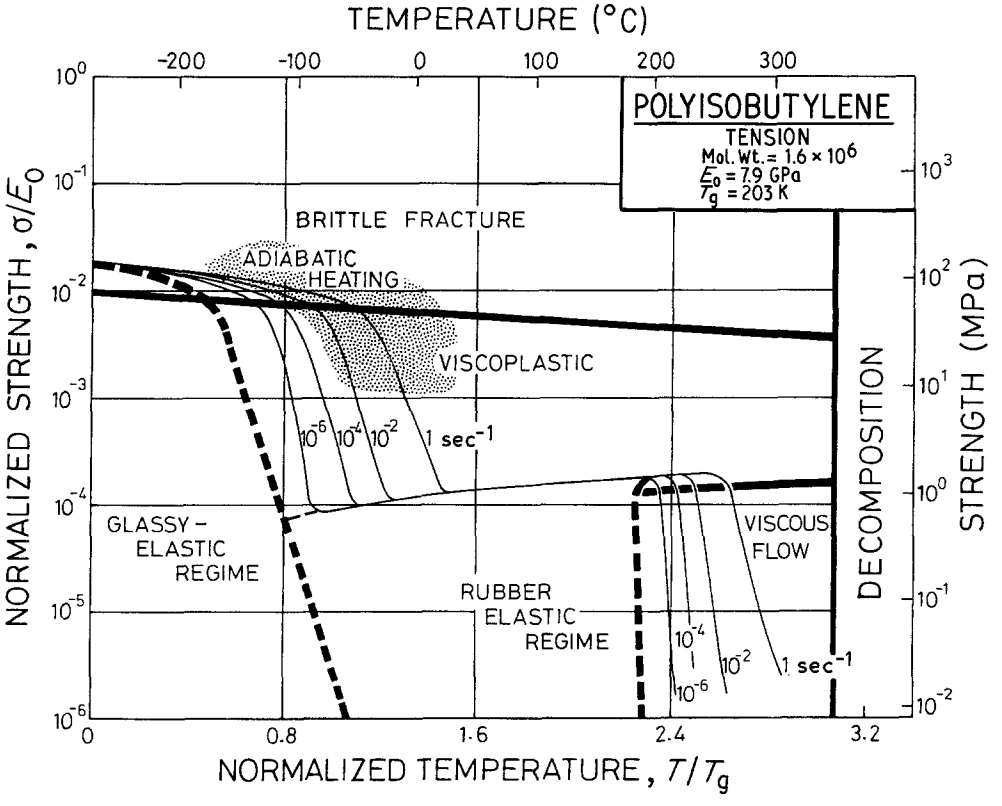

Figure 14 A failure-mechanism diagram for polyisobutylene (mol. wt. = 1.6×10^6 kg kmol^{-1}, E_0 = 7.9 GPa, T_g = 203 K) in tension. Below T_g the behaviour closely resembles that of the other polymers.

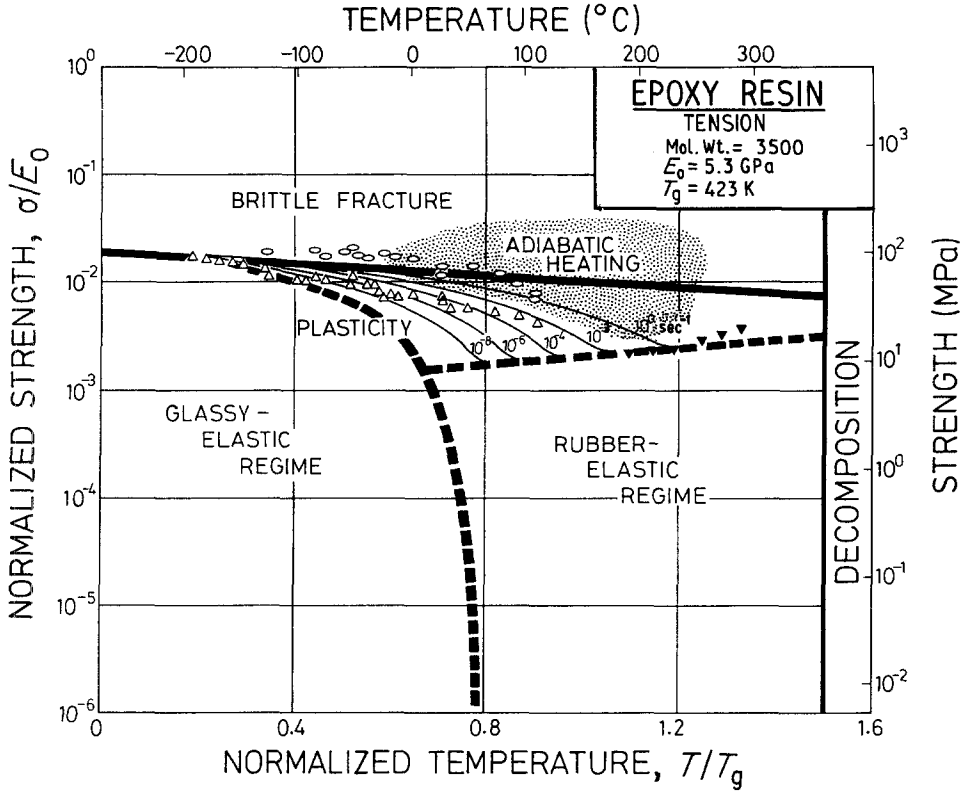

Figure 15 A failure-mechanism diagram for an epoxy resin (mol. wt. = 3.5×10^3 kg kmol^{-1}, E_0 = 5.3 GPa, T_g = 423 K) in tension. The viscous regime is suppressed by cross-linking. (△, ●) Pink and Campbell [12] (3.3×10^{-4} sec^{-1}), (▼) Kline [77].

assumed to be 1×10^5 kg k/mol^{-1}. Data for tension are those of Vincent [63], Beardmore [22], Imai and Brown [23] and Morgan and Ward [20]. For compression we have used the data of Beardmore [22]. In the viscous flow regime the stresses are calculated from the melt viscosity data of Brodynan *et al.* [75]. In tension, there is a regime of brittle fracture (with a ductile-to-brittle transition temperature that depends on strain-rate), a regime of plasticity and one of viscous flow. Compressive behaviour is characterized by the absence of the brittle fracture regime. Some scatter is expected in the correlation between the experimental results and the model derived in this work because of the differences in the molecular weight of the test samples.

Failure-mechanism diagrams for PS are shown in Figs 9 to 11. Data for tension are from Wu and Brown [25] while those for compression are from Bowden and Raha [52] and Argon *et al.* [51]. The viscous flow stresses are calculated from the melt viscosity data of Spencer and Dillon [76]. Figs 9 and 10 show the behaviour in tension corresponding to two different molecular weights. The higher molecular weight gives a larger region of plasticity and yielding, implying that higher molecular weight samples will be less brittle than those of lower molecular weights. As in the case of PMMA, brittle fracture and crazing is suppressed under compressive conditions as shown in Fig. 11.

Diagrams for PC are shown in Figs 12 and 13. For molecular weights above the critical value of 1.5×10^4 there is no indication of brittle fracture behaviour for both tension and compression. Data for both tension and compression are from Bauwens-Crowet *et al.* [26]. To locate the viscous flow regime we have used the viscosity data of van Krevelen [55].

A diagram for high molecular weight PIB is shown in Fig. 14. Like the linear polymers, it is brittle below $0.8T_g$, but this now corresponds to a real temperature of about -100° C. Above T_g, there is an extensive rubbery plateau in which we have interpreted "failure" to mean "a large elastic strain (of order unity)". It extends up to almost 200° C where viscous flow starts [11].

The final diagram (Fig. 15) is for EP in tension (we have been unable to find compression data). Cross-linking suppresses viscous flow, giving a high rubbery plateau up to decomposition.

5. Summary and conclusions

Diagrams can be constructed which summarize the mechanical response of a polymer to stress. A diagram shows the fields of dominance of each of several competing failure mechanisms. Contours on the diagram show the relationship between stress, temperature and strain rate: specifying any two of these locates a point on the diagram and allows the third to be read off.

The diagrams are constructed from approximate constitutive equations, one for each mechanism, which have been fitted to experimental data for fracture, plasticity and viscous flow, and include the variables of stress state and of molecular weight. They are plotted on normalized axes (σ/E_0 and T/T_g). Because of this, polymers with similar structures have similar diagrams: that for PMMA, for instance, is broadly typical of linear amorphous polymers; and those for PIB and EP broadly typify elastomers and cross-linked epoxies.

Acknowledgements

We wish to thank the Malay Government and the

SERC for supporting the research through a studentship and a research grant.

References

1. K. M. SINNOT, *J. Polym. Sci.* **35** (1959) 272.
2. I. V. YANNAS and R. R. LUISE, *J. Macromol. Sci. Phys.* **B21**, 443.
3. S. LOSHACK, *J. Polymer Sci.* **15** (1955) 391.
4. T. G. FOX, *J. Amer. Chem. Soc.* **80** (1958) 1768.
5. S. S. ROGERS and L. MANDELKERN, *J. Phys. Chem.* **61** (1957) 945.
6. T. G. FOX and P. J. FLORY, *J. Appl. Phys.* **21** (1950) 581.
7. K. von SCHMEIDER and K. WOLF, *Kolloid-z* **134** (1953) 149.
8. K. M. SINNOT, *Soc. Plastic Engrs. Trans.* **2** (1962) 63.
9. A. BONDI, "Physical Properties of Molecules, Crystals, Liquids and Glasses" (Wiley, New York, 1968) p. 1.
10. R. G. ARRIDGE, "Mechanics of Polymers" (Clarendon, Oxford, 1975).
11. H. BARRON, "Modern Synthetic Rubbers" (Chapman and Hall, London, 1942), p. 1.
12. E. PINK and J. D. CAMPBELL, *Mater. Sci. Eng.* **15** (1974) 187.
13. M. OCHI, H. TESAKO and M. SHIMBO, *Polymer* **26** (1985) 457.
14. A. A. GRIFFITH, *Phil. Trans. R. Soc.* **A221** (1921) 163.
15. J. P. BERRY, "Fracture", Vol. 7, edited by H. Liebowitz (Academic, New York, 1972) p. 37.
16. R. J. YOUNG, "An Introduction to Polymers" (Chapman and Hall, London, 1981) p. 1.
17. M. F. ASHBY and S. H. HALLAM, *Acta Metall.* **34** (1986) 497.
18. J. G. WILLIAMS and G. P. MARSHALL, *Proc. R. Soc.* **A342** (1975) 55.
19. G. P. MARSHALL, L. H. COUTTS and J. G. WILLIAMS, *J. Mater. Sci.* **9** (1974) 1409.
20. G. P. MORGAN and I. M. WARD, *Polymer* **18** (1977) 87.
21. R. A. W. FRASER and I. M. WARD, *ibid.* **19** (1978) 220.
22. P. BEARDMORE, *Phil. Mag.* **19** (1969) 389.
23. Y. IMAI and N. BROWN, *J. Mater. Sci.* **11** (1976) 4.
24. P. I. VINCENT, "The Encyclopaedia of Polymer Science and Technology", (Wiley, New York, 1967) p. 226.
25. J. C. B. WU and N. BROWN, *J. Mater. Sci.* **17** (1982) 1311.
26. C. BAUWENS-CROWET, J. C. BAUWENS and G. A. HOMES, *ibid.* **7** (1972) 176.
27. A. J. KINLOCH and R. J. YOUNG, "Fracture Behaviour of Polymers" (Applied Science, London, 1983) p. 43.
28. S. S. STERNSTEIN and L. ONGCHIN, *Polym. Preprint, Amer. Chem. Soc.* **19** (1969) 1117.
29. R. J. OXBOROUGH and P. B. BOWDEN, *Phil. Mag.* **28** (1973) 547.
30. E. H. ANDREWS and L. BEVAN, *Polymer* **13** (1972) 337.
31. S. RABINOWITZ and P. BEARDMORE, *Crit. Rev. Macromol. Sci.* **1** (1972) 1.
32. N. BROWN, *J. Polym. Sci., Poly. Phys. Edn* **2** (1973) 2099.
33. E. H. ANDREWS, "Fracture in Polymers" (Oliver & Boyd, London, 1968) p. 1.
34. J. C. BAUWENS, *J. Mater. Sci.* **7** (1972) 577.
35. S. RABINOWITZ, I. M. WARD and J. S. C. PARRY, *ibid.* **5** (1970) 29.
36. R. A. DUCKETT, S. RABINOWITZ and I. M. WARD, *ibid.* **5** (1970) 909.
37. I. M. WARD, *ibid.* **6** (1971) 1397.
38. Y. S. LAZURKIN and R. A. FOGELSON, *Zhur. Tech. Fiz.* **21** (1951) 267.
39. R. E. ROBERTSON, *J. Appl. Polym. Sci.* **7** (1963) 443.
40. C. CROWET and G. A. HOMES, *Appl. Mater. Res.* **3** (1964) 1.
41. C. BAUWENS-CROWET, J. C. BAUWENS and G. A. HOMES, *J. Polym. Sci.* **7** (1969) 735.
42. J. C. BAUWENS, C. BAUWENS-CROWET and G. A. HOMES, *ibid.* **7** (1969) 1745.
43. J. A. ROETLING, *Polymer* **6** (1965) 311.
44. R. N. HAWARD and G. THACKRAY, *Proc. R. Soc.* **A302** (1968) 453.
45. D. L. HOLT, *J. Appl. Polym. Sci.* **12** (1968) 1653.
46. A. S. ARGON, *Phil. Mag.* **28** (1973) 839.
47. E. J. KRAMER, *J. Polym. Sci., Polym. Phys. Edn* **13** (1975) 509.
48. U. F. KOCKS, A. S. ARGON and M. F. ASHBY, *Progr. Mater. Sci.* **19** (1975) 1.
49. I. M. WARD, "Mechanical Properties of Solid Polymers", 2nd Edn (Wiley, Chichester, 1983) p. 194.
50. C. BAUWENS-CROWET, *J. Mater. Sci.* **8** (1973) 968.
51. A. S. ARGON, R. D. ANDREWS, J. A. GODRICK and W. WHITNEY, *J. Appl. Phys.* **39** (1968) 1899.
52. P. B. BOWDEN and S. RAHA, *Phil. Mag.* **22** (1970) 463.
53. N. G. KUMAR, *Macromol. Rev.* **15** (1980) 255.
54. G. C. BERRY and T. G. FOX, *Adv. Polym. Sci.* **5** (1968) 261.
55. D. W. van KREVELEN, "Properties of Polymers" (Elsevier, Amsterdam, 1976) p. 1.
56. M. L. WILLIAMS, R. F. LANDEL and J. D. FERRY, *J. Amer. Chem. Soc.* **77** (1955) 3701.
57. J. D. FERRY, "Viscoelastic Properties of Polymers", 3rd Edn (Wiley, New York, 1983) p. 1.
58. D. G. GILBERT, Ph.D. Thesis (Engineering Department, Cambridge, UK, 1985) p. 1.
59. I. MARSHALL and A. B. THOMPSON *Proc. Roy. Soc.* **A221** (1953) 541.
60. S. W. ALLISON and J. M. WARD, *J. Appl. Phys.* **18** (1967) 1151.
61. J. R. McLOUGHLIN and A. V. TOBOLSKY, *J. Colloid Sci.* **7** (1952) 555.
62. R. F. FEDORS, *Polymer* **20** (1979) 1055.
63. P. I. VINCENT, *Plastics (Lond.)* **26** (1960) 141.
64. J. H. GOLDEN, B. L. HAMMANT and E. A. HAZELL, *J. Polym. Sci.* **42** (1964) 4787.
65. J. R. MARTIN, J. F. JOHNSON and A. R. COOPER, *J. Macromol. Sci.-Revs. Macromol. Chem.* **C8** (1972) 57.
66. W. DOLL, "Advances in Polymer Science 52/53", edited by H. H. Kansch (Springer-Verlag, Berlin, 1975) p. 8.
67. R. P. KUSY and M. J. KATZ, *Polymer* **19** (1978) 1345.
68. G. L. PITMAN and I. M. WARD, *ibid.* **20** (1979) 895.
69. P. PRENTICE, *J. Mater. Sci.* **20** (1985) 1445.
70. A. M. DONALD, *ibid.* **20** (1985) 2630.
71. J. H. GOLDEN, B. L. HAMMANT and E. A. HAZELL, *J. Polym. Sci.* **42** (1964) 4787.
72. M. DETTENMAIER, in "Advances in Polymer Science 52/53", edited by H. H. Kansch (Springer, Berlin, 1983) p. 204.
73. A. J. KINLOCH and D. L. HUNSTON, *J. Mater. Sci. Lett.* **5** (1986) 909.
74. R. P. KUSY and D. T. TURNER, *Polymer* **18** (1977) 391.
75. J. G. BRODNYAN, R. H. SHOULBERG and E. L. KELLEY, *SPE Trans.* (1964) 277.
76. R. S. SPENCER and R. E. DILLON, *J. Colloid Sci.* **4** (1949) 241.
77. D. E. KLINE, *J. Polym. Sci.* **67** (1960) 237.
78. A. M. DONALD, private communication (1986).
79. D. G. GILBERT, M. F. ASHBY and P. W. R. BEAUMONT, *J. Mater. Sci.* **21** (1986) 3194.

Received 23 March
and accepted 3 June 1987